A Topology Preserving Non-rigid Registration Method Using a Symmetric Similarity Function-Application to 3-D Brain Images

Vincent Noblet[1,2], Christian Heinrich[1],
Fabrice Heitz[1], and Jean-Paul Armspach[2]

[1] Laboratoire des Sciences de l'Image, de l'Informatique et de la Télédétection, LSIIT, UMR CNRS-ULP 7005,
Bd Sébastien Brant, BP 10413, F-67412 Illkirch Cedex, France.
{noblet,heinrich,heitz}@lsiit.u-strasbg.fr

[2] Institut de Physique Biologique, Faculté de médecine, UMR CNRS-ULP 7004,
4 Rue Kirschleger, F-67085 Strasbourg Cedex, France.
armspach@ipb.u-strasbg.fr

Abstract. 3-D non-rigid brain image registration aims at estimating consistently long-distance and highly nonlinear deformations corresponding to anatomical variability between individuals. A consistent mapping is expected to preserve the integrity of warped structures and not to be dependent on the arbitrary choice of a reference image: the estimated transformation from A to B should be equal to the inverse transformation from B to A. This paper addresses these two issues in the context of a hierarchical parametric modeling of the mapping, based on B-spline functions. The parameters of the model are estimated by minimizing a symmetric form of the standard sum of squared differences criterion. Topology preservation is ensured by constraining the Jacobian of the transformation to remain positive on the whole continuous domain of the image as a non trivial 3-D extension of a previous work [1] dealing with the 2-D case. Results on synthetic and real-world data are shown to illustrate the contribution of preserving topology and using a symmetric similarity function.

1 Introduction

Deformable – inter-subject – registration of 3-D medical images has received considerable attention during the last decade, as a key step for the construction and use of individualized or probabilistic anatomical atlases [2]. In this context, the goal of non-rigid image registration is to estimate the long-distance and highly nonlinear deformations corresponding to anatomical variability between individuals. To ensure the consistency of registration, the mapping should be continuous one-to-one in order to preserve the integrity of warped structures. This property, which also named topology preservation, is enforced by the positivity of the Jacobian of the transformation: it ensures that connected structures remain connected and that the neighborhood relationships between structures

T. Pajdla and J. Matas (Eds.): ECCV 2004, LNCS 3023, pp. 546–557, 2004.

is maintained. It also prevents the disappearance or appearance of existing or new structures. As often noticed, the topology preservation assumption may not be valid in pathological cases, for example when registering brain images with tumor appearance or when registering images before and after surgery. Although in these cases no homeomorphic transformation exists between the two images, we show here that a topology preserving registration algorithm may be used with profit to detect topology violation. Another desirable property of the registration is that the estimated transformation from image A to B should equal the inverse of the transformation from B to A. When using a standard asymmetric cost function such as the sum of squared differences (SSD), this property is seldom fulfilled, and the resulting estimated transformation depends on the arbitrary choice of the reference image.

In [3], Cachier explains why most non-rigid registration methods are asymmetric and proposes some inversion-invariant energy to symmetrize the registration problem. Ashburner also raised the problem of symmetrization in [4], but the symmetrization concerns only the prior of the Bayesian model and not the similarity criterion. Thirion [5] forces the symmetry of the registration by computing the direct deformation T_{12} (from image 1 to image 2), the reverse deformation T_{21} (from image 2 to image 1) and the residual deformation $R = T_{21} \circ T_{12}$, and then by redistributing equally the residual deformation between T_{12} and T_{21} to obtain $R \simeq Id$. By this way, the bijectivity of the deformation is enforced, but preservation of the topology on the continuous image domain is not ensured. Christensen [6] presents a consistent registration scheme by jointly estimating the forward and reverse transformations, constraining them to be inverse of each other, and restricting them to preserve topology by constraining them to obey the laws of continuum mechanics. In this paper, we present an alternative to Christensen's non-parametric continuum model, enabling fast symmetric and topology preserving registration of 3-D images on the continuous image domain. A typical warp on 128^3 images, with "good" accuracy, is computed in less than 30 minutes on a standard 2.4 GHz PC workstation. Our approach is based on a 3-D hierarchical parametric model of the deformation field using B-spline representations. The parameters of the model are estimated by minimizing a symmetric form of the SSD criterion, under the constraint of positivity of the Jacobian. This paper is a non-trivial extension of [1], which addresses the case of 2-D topology preserving mappings using asymmetric cost functions.

This paper is organized as follows. In section 2, we present the hierarchical parametric deformation model, and we detail the optimization method used to minimize a symmetric similarity criterion, subject to the positivity constraint on the Jacobian. In section 3, we illustrate the contribution of topology preservation and of a symmetric objective function on synthetic and real-world data.

2 Registration Method

In this section, we first present the parametric hierarchical deformation model. Then we deal with the mathematical issue of topology preservation and we introduce the symmetric objective function. Finally the optimization strategy for

minimizing the symmetric objective function under the constraint of topology preservation is described.

2.1 The Parametric Hierarchical Deformation Model

Let us consider two images $I_{source}(\mathbf{s})$ and $I_{target}(\mathbf{s})$ ($\mathbf{s} = [x, y, z]^t$), both defined on $\Omega \subset \mathbb{R}^3$. The goal is to find the mapping $\mathbf{h}(\mathbf{s}) = \mathbf{s} + \mathbf{u}(\mathbf{s}) \in \mathcal{H}$, where $\mathcal{H}$ is the Hilbert space of finite energy mappings and $\mathbf{u}$ the associated displacement vector field, so that the warped image $I_{source}(\mathbf{h}(\mathbf{s}))$ is as close as possible to the target image $I_{target}(\mathbf{s})$ in the sense of some similarity criterion $E(\mathbf{h})$. The vector field $\mathbf{u}$ is parameterized at different scales using a decomposition over a sequence of nested subspaces $V_0 \subset V_1 \subset ... \subset V_l \subset V_{l+1} \subset ... \subset \mathcal{H}$, defining a multiresolution approximation of $\mathbf{u}$ [7,8]. Let Φ be a scaling function. At scale l (*i.e.*, in space V_l), the displacement field $\mathbf{u}$ is parameterized by the vector of coordinates $\mathbf{a^l} = \{a^l_{x;i,j,k}; a^l_{y;i,j,k}; a^l_{z;i,j,k}\}$ as:

$$\mathbf{u}^l(x,y,z) = \begin{bmatrix} u^l_x(x,y,z) \\ u^l_y(x,y,z) \\ u^l_z(x,y,z) \end{bmatrix} = \begin{bmatrix} \sum_{i,j,k} a^l_{x;i,j,k}\ \Phi^l_{i,j,k}(x,y,z) \\ \sum_{i,j,k} a^l_{y;i,j,k}\ \Phi^l_{i,j,k}(x,y,z) \\ \sum_{i,j,k} a^l_{z;i,j,k}\ \Phi^l_{i,j,k}(x,y,z) \end{bmatrix}, \tag{1}$$

where

$$\Phi^l_{i,j,k}(x,y,z) = 2^{3l/2}\ \Phi\left(2^l x - i\right)\ \Phi\left(2^l y - j\right)\ \Phi\left(2^l z - k\right). \tag{2}$$

Only first degree polynomial spline scaling functions Φ will be addressed in this paper, but the method may easily be extended to higher degree B-spline functions [9]. This multiresolution model allows to estimate the deformation field $\mathbf{u}$ in a coarse-to-fine approach. The cost function $E(\mathbf{h})$ is minimized over each space V_l with respect to parameters $\mathbf{a^l}$, using as an initialization the parameters $\mathbf{a^{l-1}}$ estimated at the previous scale.

2.2 Topology Preservation Enforcement

As already stated, a desirable property of inter-subject medical image warping is the preservation of the topology of anatomical structures. By enforcing this constraint, the space of possible solutions is restricted to deformations satisfying the real-world property of matter.

Topology preservation is related to the continuity and invertibility of the transformation, which should be a homeomorphism, *i.e.* a one-to-one mapping. This property is enforced by the positivity of the Jacobian of the transformation. In a more general way, we will enforce the Jacobian to be bracketed between two user-defined bounds J_m and J_M on the whole continuous domain of the image, *i.e.*:

$$\forall [x,y,z]^t \in \Omega \qquad J(x,y,z) \in [J_m, J_M]. \tag{3}$$

In this framework, topology preservation becomes a particular case by setting $J_m = 0$ and $J_M = +\infty$.

Let $\Omega^l_{i,j,k}$ denote the 3-D support of the first degree spline scaling function $\Phi^l_{i,j,k}(x,y,z)$. $\Omega^l_{i,j,k}$ is partitioned into eight identical subboxes denoted $S^l_{p,q,r}$, where $p \in \{i-1;i\}; q \in \{j-1;j\}; r \in \{k-1;k\}$. The following expression of the Jacobian may be obtained on each $S^l_{p,q,r}$ (the reader is referred to [9] for details):

$$\begin{aligned} J(x,y,z,\boldsymbol{\alpha}) = {} & \alpha_1 + \alpha_2\, x + \alpha_3\, y + \alpha_4\, z + \alpha_5\, x^2 + \alpha_6\, x\, y + \alpha_7\, x\, z \\ & + \alpha_8\, y^2 + \alpha_9\, y\, z + \alpha_{10}\, z^2 + \alpha_{11}\, x^2\, y + \alpha_{12}\, x^2\, z + \alpha_{13}\, x\, y^2 \\ & + \alpha_{14}\, x\, y\, z + \alpha_{15}\, x\, z^2 + \alpha_{16}\, y^2\, z + \alpha_{17}\, y\, z^2 + \alpha_{18}\, x^2\, y\, z \\ & + \alpha_{19}\, x\, y^2\, z + \alpha_{20}\, x\, y\, z^2, \end{aligned} \tag{4}$$

where $\boldsymbol{\alpha}$ is a $S^l_{p,q,r}$-dependent function of the $\mathbf{a}^l$'s.

2.3 Definition of the Objective Function

A standard approach for estimating the parameters of the transformation addressing single modal non-rigid registration is to minimize the sum of squared differences (SSD) criterion:

$$E(\mathbf{h}) = \int_\Omega |I_{target}(\mathbf{s}) - I_{source}(\mathbf{h}(\mathbf{s}))|^2 \; d\mathbf{s}.$$

Using this similarity function requires that a reference (target) image be chosen since both images do not play symmetric roles. The choice of the reference is arbitrary. As a consequence, the estimated transformation from I_{target} to I_{source} will not be equal to the inverse of the transformation from I_{source} to I_{target}, which should be the case ideally. We introduce a modified form of the SSD criterion where both images play a symmetric role (see also [3]):

$$\begin{aligned} E_{sym}(\mathbf{h}) = {} & \frac{1}{2}\int_\Omega |I_{target}(\mathbf{s}) - I_{source}(\mathbf{h}(\mathbf{s}))|^2 \; d\mathbf{s} \\ & + \frac{1}{2}\int_\Omega \left|I_{target}\left(\mathbf{h^{-1}}(\mathbf{s})\right) - I_{source}(\mathbf{s})\right|^2 \; d\mathbf{s}. \end{aligned}$$

Thanks to the change of variable $\mathbf{v} = \mathbf{h^{-1}}(\mathbf{s})$ in the second integral term, and reminding that $d\mathbf{s} = |J(\mathbf{v})| \; d\mathbf{v}$ where J is the Jacobian of $\mathbf{h}$, we derive the following expression:

$$E_{sym}(\mathbf{h}) = \frac{1}{2}\int_\Omega (1 + |J(\mathbf{s})|)\, |I_{target}(\mathbf{s}) - I_{source}(\mathbf{h}(\mathbf{s}))|^2 \; d\mathbf{s}. \tag{5}$$

2.4 Optimization Strategy

The parameters $\mathbf{a}^l$ of $\mathbf{u}$ are updated blockwise in a Gauss-Seidel scheme: $[a^l_{x;i,j,k}; a^l_{y;i,j,k}; a^l_{z;i,j,k}]$, which affects only $\Omega^l_{i,j,k}$, are updated jointly. This strategy enables constraint (3) on the Jacobian to be handled at an acceptable computational cost. Thanks to our spline model, the partial derivatives of E with respect to the updated parameters may be expressed as:

$$\frac{\partial E_{sym}}{\partial a^l_{w;i,j,k}} = \int_\Omega \left(1 + |J(\mathbf{s})|\right) \left(I_{source}\left(\mathbf{h}\left(\mathbf{s}\right)\right) - I_{target}\left(\mathbf{s}\right)\right) \left.\frac{\partial I_{source}\left(\mathbf{v}\right)}{\partial w}\right|_{\mathbf{v}=\mathbf{h}(\mathbf{s})} \frac{\partial h_w\left(\mathbf{s}\right)}{\partial a^l_{w;i,j,k}} + \frac{1}{2}\frac{\partial |J(s)|}{\partial a^l_{w;i,j,k}} \left|I_{target}\left(\mathbf{s}\right) - I_{source}\left(\mathbf{h}(\mathbf{s})\right)\right|^2 d\mathbf{s}$$

where w stands for x, y or z. A more intricate expression is also obtained for the Hessian components (not presented here for the sake of conciseness). Therefore we implemented two methods of optimization: gradient descent and the Levenberg-Marquardt algorithm [10].

In the case of a blockwise descent scheme, condition (3) needs only be checked on the box $\Omega^l_{i,j,k}$ since the coordinates to be modified do not affect $\Omega \setminus \Omega^l_{i,j,k}$. Considering that the blockwise descent takes place along direction $\mathbf{d}$ ($\mathbf{d}$ is a coordinate vector defined on the space $\left[a^l_{x;n_1,n_2,n_3}\ a^l_{y;n_1,n_2,n_3}\ a^l_{z;n_1,n_2,n_3}\right]$) with a step δ, the expression of the Jacobian (4) on each $S^l_{p,q,r}$ may be expressed as:

$$J(x, y, z, \delta) = A(x, y, z)\delta + B(x, y, z),$$

where $A(x, y, z)$ and $B(x, y, z)$ are polynomial forms similar to (4). As a consequence, for each point $[x, y, z] \in S^l_{p,q,r}$, the Jacobian is an affine function of δ. Notice that this remains true for higher order spline functions, up to the difference that $A(x, y, z)$ and $B(x, y, z)$ are higher order polynomials [9].

Let us define:

$$\begin{cases} J_m\left(\delta\right) = \inf\limits_{[x,y,z]^t \in S^l_{p,q,r}} J\left(x, y, z, \delta\right), \\ J_M\left(\delta\right) = \sup\limits_{[x,y,z]^t \in S^l_{p,q,r}} J\left(x, y, z, \delta\right). \end{cases}$$

It can easily be shown that $J_m(\delta)$ is concave and $J_M(\delta)$ is convex as the infimum and supremum of a set of affine functions. Moreover the Jacobian values $J_m\left(0\right)$ and $J_M\left(0\right)$ also match condition (3), since they are the result of a previous optimization step enforcing this very condition. Hence, the set of admissible values of δ on box $S^l_{p,q,r}$ will be bracketed between zero and an upper bound as shown on Fig. 1. For obtaining the maximum admissible step δ^+ along $\mathbf{d}$, we have to take the minimum of all bounds computed on each $S^l_{p,q,r}$. But computing the bound on $S^l_{p,q,r}$ at an acceptable computational burden is tricky as the Jacobian $J(x, y, z)$ has no nice property of convexity and may have several local minima and maxima. Interval analysis techniques provide a good way of quickly finding a bracketing of the global minimum and maximum of the Jacobian for a given step

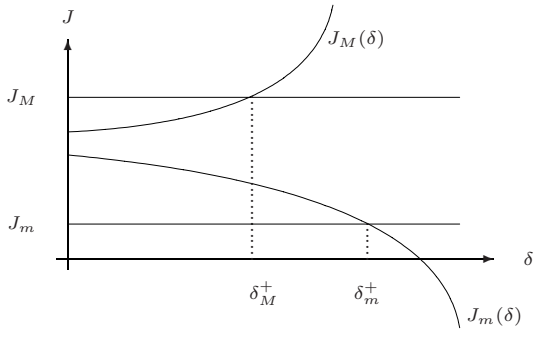

Fig. 1. The upper bound of δ on $S^l_{p,q,r}$ is computed as $\inf\{\delta_M^+, \delta_m^+\}$.

δ. So it becomes possible to quickly find a braketing of the maximum admissible step δ^+. We refer the reader to [11] for a general flavor of interval analysis and to [9] for more details on the algorithms leading to the determination of the upper bound δ^+.

3 Results

In this section we present results on synthetic and real-world data aiming at illustrating the contribution of topology preservation and of using a symmetric similarity criterion with the prospect of detecting tumors. An assessment of registration accuracy is obtained on simulated deformation fields applied on real images.

3.1 Contribution of Topology Preservation

To highlight the contribution of topology preservation, we consider the warping of an anatomical atlas, which is one of the most robust methods for performing automatic segmentation of anatomical structures. Atlas-based segmentation consists in registering a patient MRI towards a reference MRI, which is itself associated to a 3-D reference segmentation map (the atlas). The atlas is then warped on the patient data, using the estimated deformable mapping. On Fig. 2, we present the matching between two 3-D 128^3 MR brain images focusing our attention on segmented ventricles. Without topology preservation, a tearing [1] of the ventricle can be observed when the estimated deformation field is applied to the reference atlas segmentation map (Fig. 2(e)). Enforcing the Jacobian to be positive is a way of preserving the integrity of anatomical structures during the registration process (Fig. 2(f)).

[1] In fact, no tearing may happen with the transformation at hand since this deformation is necessarily continuous. Only folding is involved when topology is violated. Folding has the same visual effect as tearing.

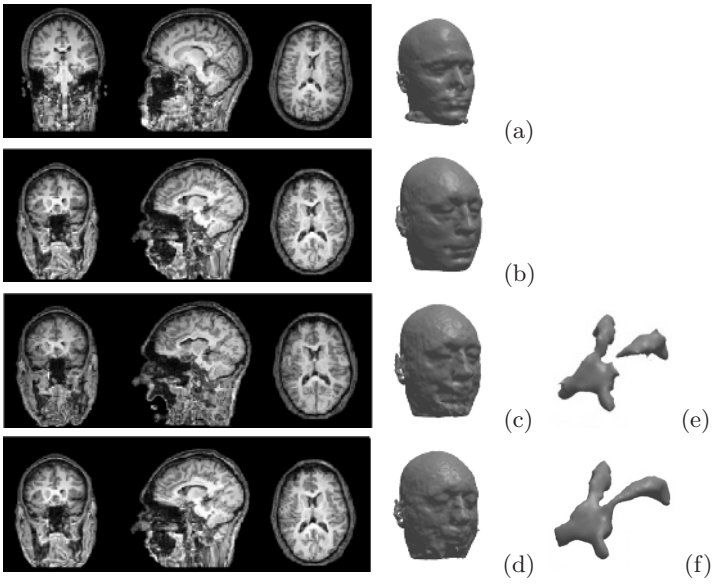

Fig. 2. 3-D non-rigid matching between two different patients and application to atlas-based ventricle segmentation: (a) source image (atlas); (b) target image (patient); (c) result of matching without any constraint; (d) result of matching with the positivity constraint $J > 0$; (e) warping of the ventricle from the atlas onto the target image (no positivity constraint); (f) warping of the ventricle from the atlas onto the target image (with positivity constraint).

3.2 Contribution of a Symmetric Similarity Criterion

The contribution of using a symmetric similarity criterion is illustrated here on a 3-D toy example involving a plain cube (Fig. 3(b)) and a second cube with a spherical hole inside (Fig. 3(a)). The goal is to show the behavior of topology preserving matching using either asymmetric or symmetric similarity criteria, when registering two volumes which are not topologically equivalent.

Let us first consider the case of registering Fig. 3(a) on Fig. 3(b). Whatever the cost function chosen (symmetric or asymmetric), the topology preserving matching algorithm tends to shrink the hole to one point, as illustrated on Fig. 3(c), which shows the effect of the deformation field applied to a synthetic grid. This shrinking of the hole yields high values of the Jacobian of the estimated transformation. This seems to be in contradiction with what we expect since a Jacobian lower (resp. higher) than 1 represents a contraction (resp. dilatation). But in the formalism presented in this paper, the warped image is obtained as $I_{warped}(\mathbf{s}) = I_{source}(\mathbf{h}(\mathbf{s}))$. This means that the small area (ideally a point) resulting from the shrinking of the hole is sent by $\mathbf{h}$ on the whole hole, corresponding indeed to a dilatation.

Now let us consider the reverse case of registering Fig. 3(b) on Fig. 3(a). Using an asymmetric SSD cost function will lead to the estimation of an identity transformation Fig. 3(d) as there is no way to decrease the value of the objec-

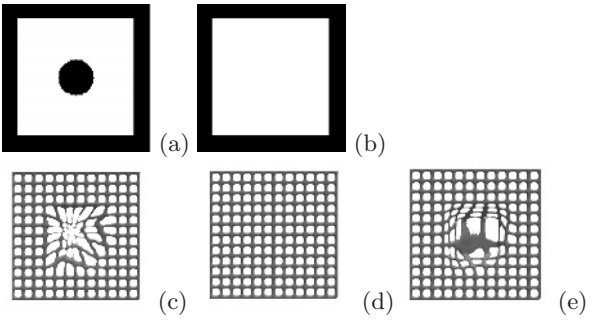

Fig. 3. 2-D slices of a 3-D toy example illustrating the contribution of using a symmetric similarity criterion: (a) plain cube with a spherical hole inside; (b) plain cube; (c) resulting transformation for a registration of (a) on (b) applied to a synthetic grid (the same result is observed when using either symmetric or asymmetric similarity criteria); (d) resulting transformation for a registration of (b) on (a) using an asymmetric similarity criterion; (e) resulting transformation for a registration of (b) on (a) using a symmetric similarity criterion.

tive function. This is not satisfactory as it means that the topology preserving registration method would be able to cope with disappearance of structures but not with appearance of new ones. Moreover this means that registering an image A on an image B and then registering B on A will lead to two transformations which are not the inverse of each other. This problem does not appear when using a symmetric cost function as E_{sym} (5). When registering Fig. 3(b) on Fig. 3(a) using E_{sym}, thanks to the term $(1 + |J|)$, the resulting deformation field tends to send as few points as possible towards the counterpart black hole, in order to assign less weight to this area in the similarity criterion . The resulting transformation (Fig. 3(e)) corresponds indeed to the inverse of the transformation represented on Fig.3(c). Thus, although there is no difference in the warped image, the use of a symmetric cost function allows to deal with the appearance of new structures, with significant consequences on the deformation field. In particular the Jacobian becomes very small at the location corresponding to the new appearing structure.

3.3 Application to Tumor Detection

The benefit of symmetric and topology preserving warping is finally illustrated on a simple simulation of tumor (or lesion) detection. To this end, we introduce a dark inclusion representing a tumor in a real 3-D MRI (Fig. 4(b)) and we register it with a healthy brain image from another patient (Fig. 4(a)). When registering Fig. 4(b) on Fig. 4(a), the topology preserving transformation matches the corresponding brain structures by shrinking the tumor to a small area (ideally a point) (Fig. 4(c)), yielding high values of the Jacobian of $\mathbf{h}$. By this way, detecting a tumor amounts to finding particularly high values of the Jacobian.

Let us now consider the reverse case of registering Fig. 4(a) on Fig. 4(b). Without the positivity constraint on the Jacobian and using the SSD criterion,

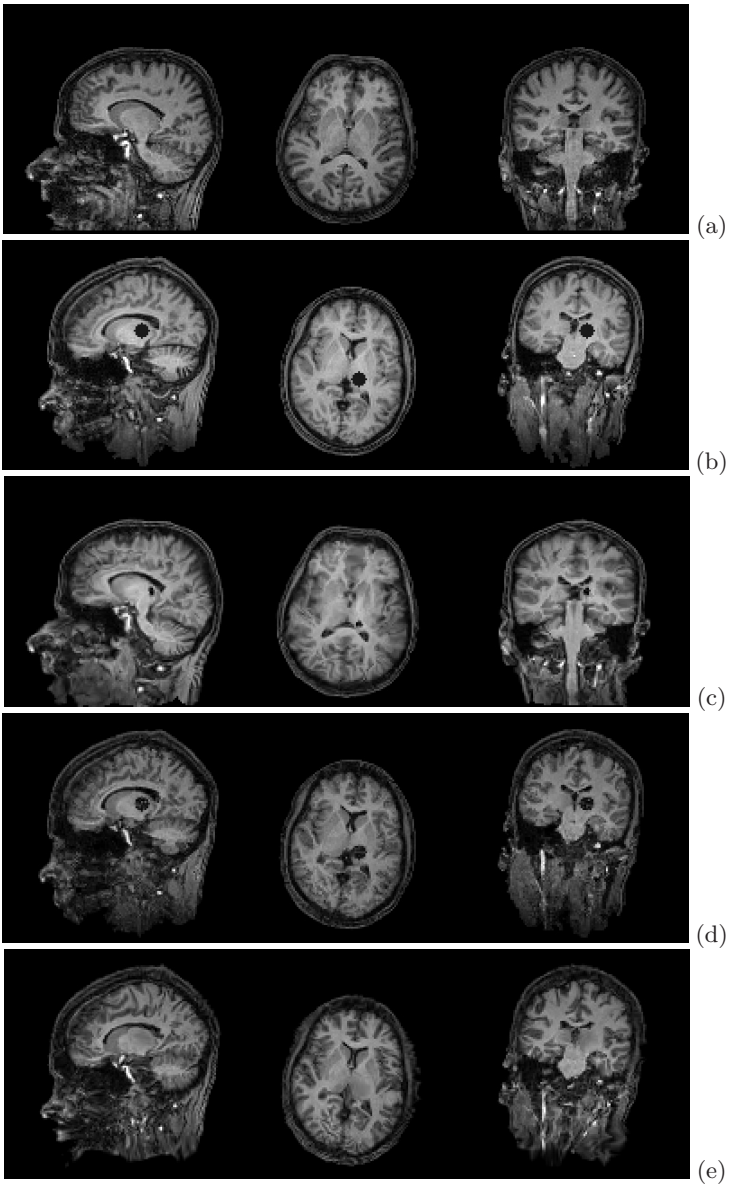

Fig. 4. Registration of two topologically different brain images: (a) normal - patient 1 - brain; (b) brain of patient 2 with a simulated tumor; (c) result of matching (b) on (a) with the symmetric similarity criterion and under the constraint of positivity of the Jacobian; (d) result of matching (a) on (b) with the symmetric similarity criterion and without the positivity constraint on the Jacobian; (e) result of matching (a) on (b) under the constraint of positivity of the Jacobian (same result with both symmetric and asymmetric similarity criteria).

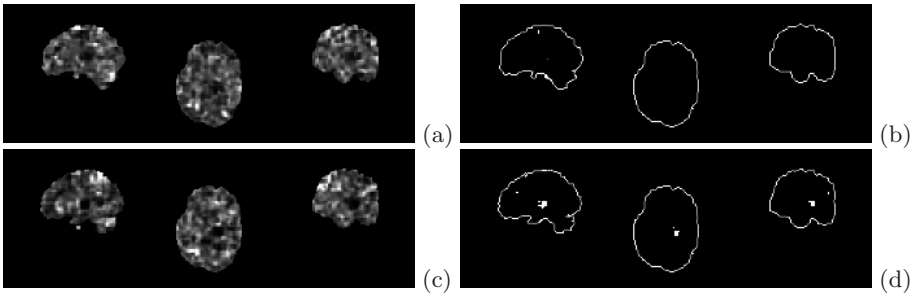

Fig. 5. Jacobian maps computed from the mapping of topologically different brain images: (a) Jacobian map (source: Fig. 4(a), target: Fig. 4(b), positive Jacobian constraint, asymmetric similarity criterion); (b) thresholded Jacobian map (no tumor is detected); (c) Jacobian map (source: Fig. 4(a), target: Fig. 4(b), positive Jacobian constraint, symmetric similarity criterion); (d) thresholded Jacobian map (tumor is detected).

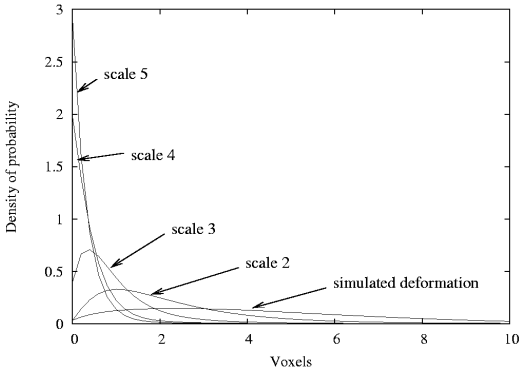

Fig. 6. Histograms of residual vector field errors computed for nine 128^3 estimated deformation fields after deformable matching at scales $L = 2, 3, 4$ and 5.

a new structure is created by the warping to match the tumor. This new structure stems from a tearing of the ventricle (Fig. 4(d)). If the positivity constraint on the Jacobian is enforced, almost nothing can be seen visually on the warped image (Fig. 4(e)). With an asymmetric similarity criterion, the Jacobian of the estimated transformation has no abnormal small values, and consequently nothing can be detected when thresholding the Jacobian map (Fig. 5(b)). On the contrary, when registering Fig. 4(a) on Fig. 4(b) with the symmetric criterion E_{sym}, very small values of the Jacobian are obtained in the critical area. In this case, the tumor can be detected by simply thresholding the Jacobian map (Fig. 5(d)). Detection of tumor may thus be achieved by registering both images (whatever the choice of the reference image) with a topology preserving mapping using a symmetric similarity criterion, and then by finding abnormal (high or low) values of the Jacobian of the estimated transformation.

3.4 Validation of 3-D Deformable Matching with Simulated Fields

Validation of non-rigid image registration is an intricate problem due to the lack of ground truth. We propose to assess the relevance of the registration algorithm by generating a ground truth using simulated transformations applied to real MRIs. To this end, we generate a transformation $\mathbf{h}_{simulated}$ with large nonlinear deformations while preserving topology, as described in the appendix. For a given real MR Image I, we register $I(\mathbf{h}_{simulated}(\mathbf{s}))$ on $I(\mathbf{s})$ with the Levenberg-Marquardt algorithm using the symmetric SSD criterion and under the positivity constraint of the Jacobian. The resulting transformation $\mathbf{h}_{estimated}$ should be compared with $\mathbf{h}^{-1}_{simulated}$. The errors between the "true" transformation and the estimated one have been evaluated using the standard $\mathcal{L}_2$ norm: $\mathcal{L}_2(\mathbf{s}) = \left\|\mathbf{h}_{estimated}(\mathbf{s}) - \mathbf{h}^{-1}_{simulated}(\mathbf{s})\right\|$. Fig. 6 shows the mean histograms of the error vector field computed for three random deformation fields applied on three different MR images. The histograms are computed at different scales ($L = 2, 3, 4, 5$). As can be seen, at scale 5, more than 96% of the voxels are affected by a quadratic error lower than one voxel.

4 Conclusion

In this paper, we have described a novel parametric modeling approach, enabling topology preservation in the registration of 3-D brain images. Topology preservation is enforced on the continuous image domain by the way of a positivity constraint on the Jacobian of the transformation. The registrations of 3-D 128^3 MR brain images are performed[2] in less than 30 minutes of CPU time on a 2.4 GHz PC workstation. We have also shown that the introduction of a symmetric form of the similarity criterion leads to a more consistent registration and paves the way to tumor detection.

References

1. Musse, O., Heitz, F., Armspach, J.P.: Topology preserving deformable image matching using constrained hierarchical parametric models. IEEE Transactions on Image Processing **10** (2001) 1081–1093
2. Toga, A., Thompson, P.: Image registration and the construction of multidimensional brain atlases. In Bankman, I., ed.: Handbook of medical imaging. Processing and analysis. Academic Press (2000) 635–653
3. Cachier, P., Rey, D.: Symmetrization of the non-rigid registration problem using inversion-invariant energies: application to multiple sclerosis. In: Proc. of MICCAI'00 - LNCS 1935, Pittsburgh, USA (2000) 472–481
4. Ashburner, J., Andersson, J., Friston, K.: Image registration using a symmetric prior - in three dimensions. Human Brain Mapping **9** (2000) 212–225
5. Thirion, J.P.: Image matching as a diffusion process: an analogy with Maxwell's demons. Medical Image Analysis **2** (1998) 243–260

[2] Registration is achieved up to scale $L = 5$, corresponding to about 90.000 parameters.

6. Christensen, G., Johnson, H.: Consistent image registration. IEEE Transactions on Medical Imaging **20** (2001) 568–582
7. Mallat, S.: A wavelet tour of signal processing. Academic Press (1998)
8. Musse, O., Heitz, F., Armspach, J.P.: Fast deformable matching of 3D images over multiscale nested subspaces. Application to atlas-based MRI segmentation. Pattern Recognition **36** (2003) 1881–1899
9. Heinrich, C., Noblet, V., Heitz, F., Armspach, J.P.: 3-D deformable image registration: a topology preservation scheme based on hierarchical deformation models and interval analysis optimization. Technical report, LSIIT, UMR CNRS-ULP 7005 (2003)
10. Rao, S.: Engineering optimization: theory and practice. third edn. Wiley-Interscience (1996)
11. Jaulin, L., Kieffer, M., Didrit, O., Walter, E.: Applied interval analysis. Springer (2001)

Appendix: Generation of a Topology Preserving Transformation

First we randomly generate a set of subboxes Ω_i, $i \in [1..N]$, defining a partition of the image Ω. To generate the partition, we randomly draw a point in the image thus defining 8 subboxes. Then for each subbox, we reiterate the operation until the size of each subbox is lower than a user-defined value. On each subbox $\Omega_i = [x_m^i, x_M^i] \times [y_m^i, y_M^i] \times [z_m^i, z_M^i]$, we define a transformation $\mathbf{h}_i$ as follows:

$$\mathbf{h}_i(x,y,z) = \begin{bmatrix} x + a_x^i sin\ \pi \left(\frac{x - x_m^i}{x_M^i - x_m^i}\right) sin\ \pi \left(\frac{y - y_m^i}{y_M^i - y_m^i}\right) sin\ \pi \left(\frac{z - z_m^i}{z_M^i - z_m^i}\right) \\ y + a_y^i sin\ \pi \left(\frac{x - x_m^i}{x_M^i - x_m^i}\right) sin\ \pi \left(\frac{y - y_m^i}{y_M^i - y_m^i}\right) sin\ \pi \left(\frac{z - z_m^i}{z_M^i - z_m^i}\right) \\ z + a_z^i sin\ \pi \left(\frac{x - x_m^i}{x_M^i - x_m^i}\right) sin\ \pi \left(\frac{y - y_m^i}{y_M^i - y_m^i}\right) sin\ \pi \left(\frac{z - z_m^i}{z_M^i - z_m^i}\right) \end{bmatrix}.$$

The resulting transformation leaves the borders of Ω_i invariant, so that preserving topology on Ω is equivalent to ensuring bijectivity of every $\mathbf{h}_i$ on each Ω_i. The set of parameters $[a_x^i; a_y^i; a_z^i]$ are randomly generated while observing the following condition:

$$(\forall \mathbf{s} \in \Omega_i \quad J_{\mathbf{h}_i}(\mathbf{s}) > 0) \Leftrightarrow \left(\frac{|a_x^i|}{x_M^i - x_m^i} + \frac{|a_y^i|}{y_M^i - y_m^i} + \frac{|a_z^i|}{z_M^i - z_m^i} < \frac{1}{\pi} \right).$$

Hence $\mathbf{h}$ is defined as: $\forall \mathbf{s} \in \Omega_i \quad \mathbf{h}(\mathbf{s}) = \mathbf{h}_i(\mathbf{s})$. In this scheme, many points in the image are left invariant by $\mathbf{h}$ since the borders of each Ω_i are invariant. Following the same approach, we thus generate a second transformation $\mathbf{h}'$ defined on another random partition of the image, and then we compose $\mathbf{h}$ and $\mathbf{h}'$ to obtain the final transformation $\mathbf{h}_{simulated}$. Finally, we compute numerically the inverse transformation $\mathbf{h}_{simulated}^{-1}$ of $\mathbf{h}_{simulated}$ while we register the warped image on the original one. The inversion is conducted by estimating for each point an interval containing its antecedent and by iteratively reducing the size of this interval until reaching the desired accuracy.